Applied Catalysis B: Environmental 219 (2017) 109–122

Contents lists available at ScienceDirect

Applied Catalysis B: Environmental

journal homepage: www.elsevier.com/locate/apcatb

p-Nitrophenol degradation by heterogeneous Fenton's oxidation over activated carbon-based catalysts

Carmen S.D. Rodrigues [a,*], O.S.G.P. Soares [b,*], M.T. Pinho [b], M. Fernando R. Pereira [b], Luis M. Madeira [a]

[a] LEPABE – Laboratório de Engenharia de Processos, Ambiente, Biotecnologia e Energia, Departamento de Engenharia Química, Faculdade de Engenharia, Universidade do Porto, R. Dr. Roberto Frias, 4200-465 Porto, Portugal
[b] Laboratório de Processos de Separação e Reação – Laboratório de Catálise e Materiais (LSRE-LCM), Departamento de Engenharia Química, Faculdade de Engenharia, Universidade do Porto, R. Dr. Roberto Frias, 4200-465 Porto, Portugal

ARTICLE INFO

Article history:
Received 10 March 2017
Received in revised form 16 June 2017
Accepted 15 July 2017
Available online 18 July 2017

Keywords:
p-Nitrophenol
Activated carbon
Adsorption
Catalytic wet peroxidation
Heterogeneous Fenton's oxidation
Surface chemical properties

ABSTRACT

Activated carbons with different surface chemical properties were used as adsorbents or as catalysts for *p*-nitrophenol (PNP, 500 mg/L) removal by adsorption or wet peroxidation processes, respectively. The surface chemical properties of the support play an important role in PNP adsorption and in the catalytic performance of the respective iron-supported catalysts. Among the series of materials prepared, which were characterized by several techniques (nitrogen adsorption at −196 °C, elemental analysis, temperature programmed desorption, pH at the point of zero charge and temperature programmed reduction), the support doped with melamine, as nitrogen precursor, and impregnated with iron (sample Fe/ACM), presents the best catalytic performance. This catalyst is stable during reutilization in five consecutive runs, without any iron leaching. A relationship between PNP removal after 1 h of reaction and the oxygen and nitrogen amount present in the carbon materials was established. A parametric study was carried out to evaluate the effect of the main operating conditions, namely temperature, pH, hydrogen peroxide concentration and catalyst dose in PNP and total organic carbon (TOC) removal. Under the best operating conditions, i.e., pH = 3.0, T = 50 °C, [H_2O_2] = 1.0 g/L (concentration below the stoichiometric amount for total degradation) and [Fe/ACM] = 2.0 g/L, 94, 90 and 86% of PNP, TOC and chemical oxygen demand (COD) removals were achieved after 2 h of Fenton's reaction, respectively, generating a non-toxic effluent with enhanced biodegradability.

1. Introduction

p-Nitrophenol (PNP) is widely used in the manufacture of drugs, explosives, dyes and fungicides [1], and is a pollutant typically present in industrial wastewaters. It is very toxic (LD_{50} = 250 mg/kg [2]), mutagenic and carcinogenic and regarded as a priority pollutant by US EPA [3]. High levels of PNP have been found in water courses; for example, a concentration of 60 μg/L was reported in drinking water [2]. Thus, to minimize the impact on the environment and in the human health is priority to remove PNP from wastewater before discharge.

Several treatment technologies have been studied for PNP removal, such as adsorption [4,5], biological degradation [6,7] and electrochemical treatment [8,9]. Nevertheless, the adsorption only transfers the pollutant from one phase to another, the biological degradation treatments are inefficient or present slow degradation rates for this type of compounds [10,11], and the electrochemical processes have high operatory costs that remarkably limit their wide application in large scale [12]. The application of the Fenton process minimizes the disadvantages of these treatment techniques, reducing the contamination levels through the destruction of the organic pollutants via highly oxidative hydroxyl radicals (with high oxidation potential, 2.8 eV [13]) and ultimately promoting their conversion into carbon dioxide (CO_2) and water (H_2O); in the case of the PNP oxidation, the nitrite released into the solution from the PNP molecule is rapidly oxidized to nitrate that reacts with H^+ generating nitric acid [14]. The Fenton reaction, which is based on the decomposition of hydrogen peroxide catalyzed by iron ion, in acid environment, is described by the simplified Eqs. (1)–(3) [15,16]; Eq. (1) describes the reaction of hydroxyl radical production by decomposition of hydrogen peroxide in presence of Fe^{2+} and

* Corresponding authors.
E-mail addresses: csdr@fe.up.pt (C.S.D. Rodrigues), salome.soares@fe.up.pt (O.S.G.P. Soares).

http://dx.doi.org/10.1016/j.apcatb.2017.07.045
0926-3373/

Eq. (2) represents the catalyst regeneration reaction (i.e. reduction of Fe^{3+} to Fe^{2+} while yielding perhydroxyl radicals, which are less oxidative species). Finally, Eq. (3) represents the oxidation of the organic species (parent compound and/or intermediates).

$$Fe^{2+} + H_2O_2 \rightarrow Fe^{3+} + HO^{\bullet} + OH^{-} \quad (1)$$

$$Fe^{3+} + H_2O_2 \rightarrow Fe^{2+} + HO_2^{\bullet} + H^{+} \quad (2)$$

$$HO^{\bullet} + \text{organic matter} \rightarrow \text{oxidation products} \quad (3)$$

The Fenton process presents some advantages, such as the possibility of operation under mild conditions of pressure and temperature; moreover, it requires a relatively simple set-up and is a "green" technology (since uses non-toxic substances and the hydrogen peroxide in excess self-decomposes into inoculum compounds – water and oxygen). However, the homogeneous process has several disadvantages, namely the need of a high amount of iron ions (about 50–80 ppm) in solution, and the need to remove/recover the catalyst at the end of the process, which requires the inclusion of another stage in the treatment making the process more expensive and complex. In addition, chemical sludge generated also needs treatment. These drawbacks can be overcome by using heterogeneous catalysts, i.e., the iron species (or transition metals) supported on a porous solid matrix, so called heterogeneous Fenton-like process [17,18].

The principles of the heterogeneous Fenton-like reaction are the same of the homogeneous one, but due to the adsorption and catalysis phenomena the process becomes more complex. Eqs. (4) and (5) present the main reactions involved:

$$X\text{-}Fe^{2+} + H_2O_2 \rightarrow X\text{-}Fe^{3+} + OH^{-} + HO^{\bullet} \quad (4)$$

$$X\text{-}Fe^{3+} + H_2O_2 \rightarrow X\text{-}Fe^{2+} + HO^{\bullet} + H^{+} \quad (5)$$

where X represents the porous solid matrix.

The aim of this work is to study the catalytic oxidation of PNP using activated carbons with different surface chemistry properties as catalysts (wet peroxidation process) or as supports of iron-based catalysts. Carbon materials have been widely used as adsorbents and as catalysts (or catalyst supports), namely in AOPs, and several works have demonstrated that the surface chemical properties play an important role during the oxidation of organic compounds [19–21]. Although the use of iron supported on activated carbon has been previously reported as catalyst for degradation of several pollutants by the heterogeneous Fenton oxidation [18,22–24], to the best of our knowledge there are no works in the literature using iron supported in activated carbons with different surface chemical properties in the heterogeneous Fenton's reaction for PNP degradation. The authors found studies that use zero-valent iron on silica [11], magnetite/silica microspheres [25], magnetic Fe^0/Fe_3O_4/coke composite [26], Au-polypyrrole/fly ash composite microspheres [27] and Ti, Cr, Mn, Co and Ni on magnetite [28] as catalysts for PNP degradation. Therefore, in this work, a commercial activated carbon was modified by chemical (oxidation with nitric acid and doping with nitrogen precursors) and thermal treatments in order to obtain supports with different surface chemistries, while maintaining the original textural properties as far as possible. Other objectives of this work were to assess the catalysts stability and to optimize the process by evaluating the effect of each operating condition, while demonstrating the radicalar nature of the process involved via hydroxyl radicals, which has never been addressed in the literature.

2. Materials and methods

2.1. Materials

The PNP used was supplied by Sigma Aldrich (chemical formula $C_6H_5NO_4$, molecular weight 155.11 g/mol). A commercial activated carbon, NORIT GAC 1240 Plus, was used as starting material for the preparation of all supports/iron catalysts (iron content <0.01 wt.%). Nitric acid (65 wt.%) and iron (III) nitrate nonahydrate (>98 wt.%) were obtained from Sigma-Aldrich. Urea (99.5 wt.%) was obtained from Acros Organics, melamine (>99 wt.%) was purchased from Fluka and ethanol (96 wt.%) was obtained from JMGS.

2.2. Activated carbon functionalization

Initially, the activated carbon was crushed and the particles between 0.1 and 0.3 mm were used as starting material (sample called AC). Then, sample AC was modified by chemical and thermal treatments to obtain materials with different textural and chemical properties.

The activated carbon (AC) was oxidized with HNO_3 in a 125 mL Soxhlet extraction apparatus containing 9 g of AC connected to a boiling flask and to a condenser. A volume of 300 mL of 6 M HNO_3 was introduced into a 500 mL round-bottom flask and heated to the boiling temperature with a heating mantle. The reflux was stopped after 3 h and the oxidized AC was extensively washed with distilled water to neutral pH and then dried in an oven at 110 °C overnight (sample ACH).

Afterwards, sample ACH was used as the starting material for the preparation of samples by gas-phase thermal treatments. Thermal treatments at different temperatures were carried out to selectively remove the oxygen surface groups present in the starting material. Samples ACH_{400}, ACH_{600} and ACH_{900} were obtained by heat treating sample ACH at 400, 600 and 900 °C, respectively, under nitrogen flow during 1 h.

N-doped samples were also prepared from the commercial AC using two different N-precursors: urea and melamine. For that, 0.6 g of the original AC was dipped into 50 mL of a 1 M aqueous solution, using water in the case of urea and ethanol 96% in the case of melamine, and stirred at room temperature during 24 h. Thereafter, the samples (ACU and ACM) were filtered, washed with distilled water and dried in an oven at 110 °C overnight. These samples were heat treated at 600 °C during 1 h under nitrogen flow.

2.3. Catalysts preparation

Iron catalysts supported in all the carbon materials were prepared by the incipient wetness impregnation method. The impregnation was carried out under vacuum and ultrasonic mixing. The precursor solution was prepared with iron (III) nitrate nonahydrate in order to obtain an iron load of 2 wt.%; the iron content in the catalysts should be very similar to the theoretical, as verified in previous works using the same methodology [29]. After impregnation, the samples were dried at 110 °C overnight and heat treated at 400 °C during 1 h under nitrogen flow and reduced under hydrogen flow for 3 h at 400 °C (Fe/ACX_y).

Table 1 summarizes the preparation methods of the carbon samples.

2.4. Supports and catalysts characterization

The supports (all activated carbon-based materials without iron) were characterized by N_2 adsorption at −196 °C, elemental analysis, temperature programmed desorption (TPD), determination of pH at the point of zero charge (pH_{PZC}) and the iron-based

Table 1
Abbreviations of the samples and description of the treatments applied.

Abbreviation	Starting material	Description of treatment
AC	Original	None
ACH	Original	Oxidation in liquid phase with 6 M HNO_3
ACH_{400}	ACH	Thermal treatment under N_2 flow at 400 °C
ACH_{600}	ACH	Thermal treatment under N_2 flow at 600 °C
ACH_{900}	ACH	Thermal treatment under N_2 flow at 900 °C
ACU	Original	N-doping with urea
ACM	Original	N-doping with melamine
Fe/ACX_y	Modified activated carbons	Incipient wetness impregnation method

X_y: represents the modification conducted on the different samples.

catalysts were also characterized by temperature programmed reduction (TPR).

The textural characterization of the samples was based on the N_2 adsorption isotherm, determined at −196 °C with a Quantachrome NOVA 4200e equipment. The samples (~0.1 g) were outgassed at 150 °C for 3 h under vacuum. The surface area (S_{BET}) of the carbon materials was calculated by the Brunauer-Emmett-Teller (BET) equation. The mesopore surface area (S_{meso}) and the micropore volumes (V_{micro}) were calculated by the *t*-method. The total specific pore volume (V_p) was determined from the amount adsorbed at $P/P_0 = 0.95$.

The amounts of carbon, hydrogen, nitrogen and sulphur were determined using a Carlo Erba EA 1108 Elemental Analyzer. Ash content was determined by thermogravimetric analysis (TGA) using a Netzsch STA 409 PC equipment. The samples were heated under a helium flow from 50 to 900 °C, at a heating rate of 10 °C min^{-1} using two isothermal steps: 7 min with helium and 13 min with air. Oxygen was determined by difference.

The surface chemistry was characterized by temperature programmed desorption (TPD). The CO and CO_2 profiles were obtained with a fully automated AMI 300 apparatus (Altamira Instruments) connected to a Dycor Dymaxion Mass Spectrometer. Each sample (~0.1 g) was heated up to 1100 °C at 5 °C min^{-1} using a constant flow rate of helium equal to 25 cm^3 (STP) min^{-1}. The mass signals $m/z = 28$ and 44 were monitored during the thermal analysis. CO and CO_2 were calibrated at the end of each analysis with the respective gases.

The pH at the point of zero charge (pH_{PZC}) was determined by mixing 0.05 g of each carbon material with 25 mL of NaCl solution (0.01 M). The pH was adjusted with HCl or NaOH solutions (0.01 M), in order to obtained values between 2 and 12. The final pH was measured after 24 h under stirring at room temperature. The pH_{PZC} value of each carbon sample was determined when the curve pH_{final} vs. $pH_{initial}$ crosses the line $pH_{final} = pH_{initial}$.

TPR profiles were obtained with a fully automated AMI 200 apparatus (Altamira Instruments) and the hydrogen consumption was monitored by a thermal conductivity detector (TCD). Each sample (~0.1 g) was heated up to 600 °C at 5 °C min^{-1} under 5% (v/v) H_2-Ar at 30 cm^3 (STP) min^{-1}.

2.5. Adsorption and reaction experiments

The experiments were carried out in a slurry batch reactor, where 200 mL of PNP solution (500 mg/L) was added; the concentration used is typical of industrial effluents [10,30]. The reactor has a recirculating water jacket, linked to a thermostatic bath (Hubber, polystat cc1) to maintain the temperature constant at ±1.0 °C. After the solution has reached the desired temperature, pH was adjusted to the desired value (with 1 M sulfuric acid, from Labchem); then the support (ACX_y) was added, being this the time considered as zero for the adsorption experiments. In adsorption and reaction experiments, the initial instant (t = 0 min) coincides with the insertion of the desired hydrogen peroxide (30%, LabChem) dose, immediately after the catalyst (Fe/ACX_y) or support (ACX_y). During the experiments, stirring (200 rpm) was ensured using a magnetic stir bar and a stir plate (VWR, model VS-C7).

During the adsorption and reaction processes samples (2.5 mL) were taken along time for measuring the concentration of PNP, intermediate by-products and TOC. Before these analysis samples were filtered through a 0.2 μm nylon syringe filter (WVR) to remove the support or catalyst, while residual hydrogen peroxide was eliminated by raising the pH to 10 through the addition of 10 M NaOH (from Merck); then the samples were neutralized (to pH ~7.0) with 1 M H_2SO_4 (by Labchem). At the end of the reaction runs the residual hydrogen peroxide and iron leaching were also determined after filtration. For optimized experimental conditions, and after filtering and stopping the reaction with the same procedure described above, COD, BOD_5, carboxylic acids content, toxicity and biodegradability of the treated solution were also assessed after 2 h of oxidation.

The runs without PNP (blank runs) were carried out under the same conditions as Fenton's reaction experiments, but using only 200 mL of distilled water. The residual hydrogen peroxide and the presence of hydroxyl radicals, after filtration, were also evaluated along the reactions.

2.6. Analytical methods

The concentrations of *p*-nitrophenol and the presence of intermediate by-products (benzoquinone, *p*-nitrocatecol and hydroquinone) were assessed by high performance liquid chromatography (HPLC, Hitachi Elite LaChrom), the apparatus being equipped with a UV detector and using a Purospher STAR RP-18 column (5 μm, 250 × 4.0 mm) heated up to 35 °C. Isocratic methods were employed and the eluent (90% water and 10% methanol) flow rate was 0.75 mL/min. The detection was performed by UV absorbance at a wavelength of 285 nm for *p*-nitrophenol and 270 nm for the other compounds; the automatic injection volume was 20 μL. The quantification of carboxylic acids, namely maleic, pyruvic, oxalic and acetic acids, was carried out by HPLC using a Rezex ROA-Organic Acid H+ (8%) (250 × 4.6 mm) column and the elution was carried out with H_2SO_4 2.5 M with a flow rate of 0.17 mL/min. Injection was made with 15 μL of samples and working at 25 °C.

Total organic carbon (TOC) (difference between total carbon – TC – and inorganic carbon – IC) was measured in a Shimadzu TOC-L (Method 5310 D) [31] apparatus with autosampler (Shimadzu SHL).

Hydrogen peroxide was measured following the method developed by Sellers [32]. This method quantifies the yellow-orange color of the complex formed from the reaction of hydrogen peroxide with titanium oxalate. For that, the absorbance at 400 nm was measured in a Thermo Electron Corporation model Helios γ spectrophotometer.

The presence of hydroxyl radicals in solution was evaluated in accordance with the method proposed by Wang et al. [33]. In this method, 1,5-diphenyl carbazide (Sigma Aldrich) was oxidized by

Table 2
Textural properties of the carbon materials.

	Sample	S_{BET} (±10 $m^2 g^{-1}$)	S_{meso} (±10 $m^2 g^{-1}$)	V_{micro} (±0.01 $cm^3 g^{-1}$)	$V_{P/Po=0.95}$ ($cm^3 g^{-1}$)
Supports	AC	824	196	0.286	0.492
	ACH	704	126	0.296	0.426
	ACH_{400}	740	180	0.252	0.431
	ACH_{600}	746	195	0.253	0.456
	ACH_{900}	789	192	0.271	0.472
	ACU	820	196	0.285	0.489
	ACM	730	174	0.229	0.408
Catalysts	Fe/AC	807	179	0.288	0.479
	Fe/ACH	701	117	0.275	0.459
	Fe/ACH_{400}	704	177	0.230	0.472
	Fe/ACH_{600}	737	185	0.251	0.446
	Fe/ACH_{900}	771	189	0.267	0.467
	Fe/ACU	768	178	0.271	0.453
	Fe/ACM	717	171	0.251	0.408

hydroxyl radicals into 1,5-diphenyl carbazone that absorbs in the wavelength of 563 nm.

Iron leached to the solution was measured by flame atomic absorption spectrometry – Method 3111B [31] – using an AAS UNICAM spectrophotometer (model 939/959). Firstly, the samples were filtered through nylon filters with 0.45 μm of porosity and acidified with concentrated nitric acid till pH ~1.0 to keep iron dissolved.

Biological oxygen demand after 5 days (BOD_5) was measured according to method 5210 D [31], using an OxiTOP (Velp Scientifica) apparatus. Chemical oxygen demand (COD) was determined by the acidic digestion (closed reflux) method at 150 °C for 2 h (Thermoreactor TR 300 from Merck), using potassium dichromate as oxidant, followed by measuring the absorbance (Spectroquant Nova 60) corresponding to the reduced chromium – Method 5220 D [31].

The toxicity of the samples was quantified by inhibition of *Vibrio fischeri (V. fischer*i). In this test the bacteria was put in contact with effluent samples at 15 °C and the bioluminescence was measured after a contact time of 5, 15 or 30 min in a Microtox (Modern Water, model 500) equipment [34].

All analytical determinations were performed in duplicate and the coefficients of variation were less than 2% for TOC and PNP, 3% for COD, 7% for BOD_5, 4% for inhibition of *V. fisheri* and 1% for the hydrogen peroxide and hydroxyl radicals determination methods.

3. Results and discussion

3.1. Carbon materials characterization

3.1.1. Textural properties

Table 2 summarizes the textural properties of the different iron-containing catalysts and corresponding supports. The original AC presents the highest BET surface area (824 $m^2 g^{-1}$), whereas ACH sample shows a decrease in the surface area that is mainly related to the large amount of oxygen surface groups introduced by the treatment with nitric acid (HNO_3), which may in some extent block the access of N_2 molecules inside the small pores [19,35]. On the other hand, the heat treated supports show a small increase in the BET surface area, when compared to the sample oxidized with nitric acid, due to the thermal treatment that selectively removes some of the oxygen surface groups [19,36]; moreover, such increase in the BET surface area is more pronounced as the temperature used in the treatment increases. The N-doping with melamine provokes a reduction of the BET surface area, whereas when urea is used as N-precursor no significant differences were observed as compared to the AC sample, because the former sample material presents a large amount of N-surface groups that may partially block the access of N_2 molecules to the small pores [37].

Table 3
Elemental analysis of the different carbon supports.

Sample	C (wt.%)	H (wt.%)	N (wt.%)	S (wt.%)	O (wt.%)[a]
AC	84.6	0.17	0.45	0.73	7.23
ACH	80.1	0.12	0.86	0.55	14.9
ACH_{400}	82.2	0.13	1.51	0.32	8.99
ACH_{600}	83.3	0.12	1.07	0.36	7.18
ACH_{900}	83.7	0.11	1.74	0.38	5.14
ACU	84.2	0.11	1.76	0.40	4.53
ACM	82.5	0.12	3.44	0.48	5.57

[a] Determined by difference.

In general, the impregnation with iron did not change substantially the surface area and total pore volume of the supports. However, the iron species can occupy some space in the pores or even block the small pores [38], slightly decreasing the BET surface area.

3.1.2. Elemental analysis

Table 3 summarizes the carbon, hydrogen, nitrogen, sulphur and oxygen contents (the oxygen content was obtained by difference discounting the ashes amount) of the carbon supports. Sample ACH presents the highest amount of oxygen as a consequence of the oxidation with HNO_3. However, the oxygen content decreased from 14.9% to 5.14% with the increase of the temperature during the thermal treatments of the supports, in agreement with previous studies [39,40]. The N-doping decreases the content of oxygen (as compared to the AC sample), because some of the oxygen-containing groups are replaced by nitrogen-containing groups [39]. The highest amount of N-groups was obtained when melamine was used as N-precursor, which must be related to the amount of nitrogen in the precursor (67% in melamine and 47% in urea) [41]. On the other hand, the nitrogen content in samples oxidized and thermally treated is attributed to the formation of some nitrogen-containing groups on the carbon surface during the oxidation with nitric acid [42].

3.1.3. Temperature programmed desorption and pH_{PZC}

The total amount of the different oxygenated surface groups on the carbon supports was determined taking into consideration the amount, the decomposition temperature and the type of gas released (CO and/or CO_2) during the TPD experiments [36,43] and are shown in Table 4. Accordingly, the TPD profiles of the different carbon supports were deconvoluted into five components: carboxylic acids, carboxylic anhydrides, lactones, phenols, carbonyls or quinones. The CO_2 peaks result from the decomposition of carboxylic acids at low temperature (200–450 °C), lactones at higher temperatures (600–800 °C) and carboxylic anhydrides at intermediate temperatures (400–600 °C). The CO peaks result

Table 4
Surface chemistry of the carbon supports (total amount of CO and CO_2 released, oxygen content and pH_{PZC}).

Sample	CO (±20 μmol g^{-1})	CO_2 (±20 μmol g^{-1})	O[a] (wt.%)	pH_{PZC} (±0.1)
AC	379	173	1.2	7.7
ACH	1821	882	5.7	2.5
ACH_{400}	1436	281	3.2	6.8
ACH_{600}	1184	177	2.5	7.3
ACH_{900}	320	167	1.0	7.5
ACU	335	127	0.9	7.8
ACM	300	168	1.0	7.5

[a] Mass percentage of oxygen on the surface, obtained from TPD data assuming that all the surface oxygen is released as CO and/or CO_2.

from the decomposition of carboxylic anhydrides at intermediate temperatures (400–600 °C), phenol at slightly high temperatures (600–800 °C) and carbonyl/quinone groups at high temperatures (750–1100 °C) [36,43]. The original sample (AC) does not have significant amounts of oxygenated surface groups. The oxidation with nitric acid originates a large amount of oxygen surface groups which is shown by the increase of CO and CO_2 released (Table 4). As a result, the sample ACH presents a large amount of carboxylic acid groups, lactones and some carboxylic anhydrides, whereas phenol groups and carbonyl/quinone groups are also present. After the heat treatments at different temperatures, the carbon samples show a decrease in the amounts of CO and CO_2 released, due to the progressive removal of the oxygen surface groups during the thermal treatments. The amount of the acidic groups considerably decrease after thermal treatments above 400 °C; but the phenol and carbonyl/quinone groups only decrease significantly after heat treatment above 700 °C and practically all CO and CO_2 releasing groups were removed after treatment at 900 °C. The amounts of CO and CO_2 released by TPD for the original and N-doped samples are quite similar (see Table 4).

The mass percentage of oxygen on the surface, obtained from TPD analysis (assuming that all the surface oxygen is released as CO and/or CO_2), shown in Table 4, presents the same tendency observed for oxygen calculated by elemental analysis (Table 3).

Table 4 also shows the pH_{PZC} values of the carbon samples, wherein the original AC presents approximately neutral properties. Sample ACH has the lowest pH_{PZC} value due to the introduction of large amount of oxygen surface groups having acidic properties, mainly carboxylic acids. The heat treated samples exhibit a surface basicity consistent with the removal of the oxygen surface groups, i.e. these samples show more basic properties that follow the trend of the treatment temperature. The N-doped materials present pH_{PZC} values approximately neutral or slightly basic.

3.1.4. Temperature programmed reduction

Temperature programmed reduction (TPR) experiments were carried out to study the reduction behavior of the metal species supported on the different samples [44]. Fig. 1 shows the TPR profiles of the iron catalysts on the different supports. The position, width and intensity of the iron reduction peaks mainly depend on the nature of the supports. The major reduction peak is located at a temperature around 400 °C, and for that reason this temperature was selected for the calcination and reduction steps performed during the preparation of the catalysts. The catalyst Fe/ACH shows a wide reduction peak, which must be related to a higher interaction between iron and oxygen surface groups formed during the oxidation treatment, mainly carboxylic acids [19,45]. The catalysts supported on the thermally treated samples show a reduction peak slightly shifted to the left. For instance, the catalyst supported on the ACH_{900} sample presents a main reduction peak at around 370 °C, which must be associated with the lower amount of surface groups [19]; thus, the electrostatic interactions between negatively charged oxygen

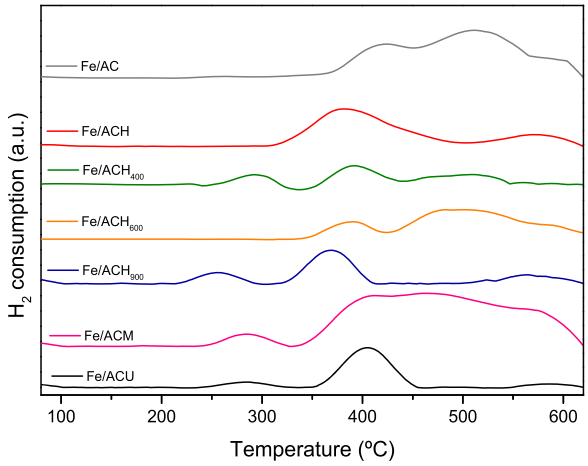

Fig. 1. TPR profiles of the iron catalysts supported on different carbon materials.

groups and iron are lesser [46]. The second peak observed above 500 °C in all carbon material profiles could be related to interaction of iron oxide with the support [41], i.e., with the temperature increase the iron species (e.g.: Fe_2O_3) are reduced to new species (e.g.: Fe_3O_4) [47]. The reduction peak of the N-doped samples is shifted to higher temperatures, indicating that the reduction temperature depends on the degree of interaction between the active species and the support [41].

3.2. Adsorption vs. reaction

Adsorption experiments were performed using the activated carbon supports to evaluate the effect of their surface chemistry on PNP adsorption and TOC reduction. As expect, a reduction of PNP and TOC concentration was observed due to adsorption (see Fig. 2a and b), which is mainly related to the high BET surface area (704–824 m^2/g – see Table 2) of the carbon materials (similar results with all samples for PNP and TOC removals indicate there is only adsorption). The results show that the surface chemical properties play an important role in the adsorption experiments, since there are not important differences between the textural properties of all the samples. The lowest PNP removal was observed for the ACH sample, which is the sample with the highest amount of oxygen surface groups and lowest pHpzc (Table 4). As the heat treatment temperature increases the oxygen-containing surface groups are progressively removed, improving the adsorption capacity of these carbon samples (from ACH to ACH_{900}). Therefore, the difference in adsorption capacities must be mainly attributed to the carbon surface that is negatively charged in the sample ACH (pH_{pzc} is lower than the pH of the solution – 3.0), due to the high amount of oxygen containing surface groups, so that the anionic PNP will suffer repulsion forces when the pollutant approaches the carbon surface. The reduction of adsorption capacity of organic pollutants for activated carbons functionalized with nitric acid has been reported in literature [19,48].

The adsorption capacity of the heat treated carbons increases with the temperature of the thermal treatment due to the decrease of the amount of oxygen-containing groups on the carbons surface (see Tables 3 and 4 for the percentage of O and amounts of CO and CO_2, respectively) which, consequently, favors the electronic interactions between the carbon surface and PNP, since the π electrons region in the basal plane of carbon predominates when there is less oxygenated surface groups [49]. Among the heat treated carbons, the highest PNP adsorption and TOC removal were observed for ACH_{900} sample that achieved 37.1 and 34.3%, respectively, after 120 min. However, the best performances for PNP adsorption (and

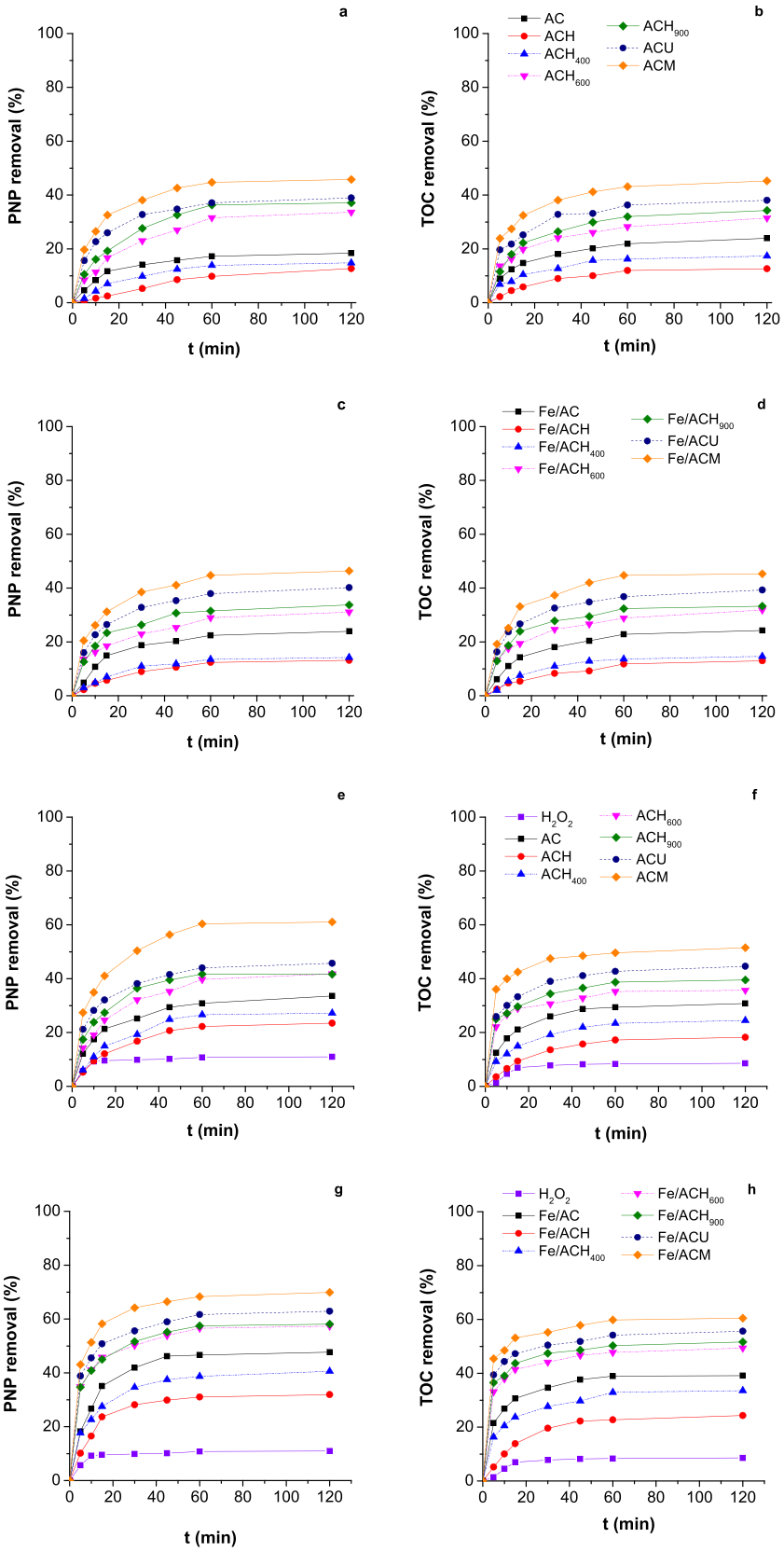

Fig. 2. PNP and TOC removal during adsorption with supports (a, b) and catalysts (c, d), wet peroxidation (e, f) and Fenton's reaction (g, h) (pH = 3.0, T = 30 °C, [support or catalyst] = 0.25 g/L, [H_2O_2] when used = 1.0 g/L, [PNP] = 500 mg/L).

TOC removal) were reached with the carbon samples doped with nitrogen, the highest removal being obtained for the carbon sample with the highest nitrogen content (ACM – see Table 3). This improvement in the adsorption of the model compound is due to the presence of N-containing groups on the carbon surface that increases the electronic density, and thus a strong interaction between PNP and the carbon surface occurs [50]. The same tendency was observed in adsorption runs in the presence of catalysts, PNP removal (and TOC reduction) obtained being similar to that reached with the supports (see Fig. 2c and d). This result is in accordance with the expected trend since the catalysts and supports present similar BET surface areas (see Table 2).

After evaluation of the activated carbons adsorption capacity the catalytic activity of the supports was also assessed. With that purpose, several experiments were performed under the same operation conditions used for the adsorption experiments, but adding hydrogen peroxide. Fig. 2e and f present the PNP and TOC removal profiles during the experiments in the presence of hydrogen peroxide. Hydrogen peroxide by itself provides a very low PNP (11.0%) and TOC (8.5%) removal, after 2 h of reaction, due to its low oxidation potential. In the presence of carbon samples and hydrogen peroxide the same tendency obtained during the adsorption experiments was observed, i.e., the acid carbon ACH presents the worst performance, as reported in other works [19,51], and the efficiency increased with the temperature used in the thermal treatment of the carbon samples. Once again, the highest removal was reached with the carbon doped with melamine (ACM). The PNP and TOC removals were slightly higher when the activated carbons were used as catalysts in wet peroxidation (WPO) than when used as adsorbents. For instance, for the ACM sample 37.1 and 34.3% for PNP and TOC removals, respectively, were achieved after 2 h by adsorption (without H_2O_2) – Fig. 2a and b, while 61.1% for PNP and 51.5% for TOC were reached by WPO (with H_2O_2) – see Fig. 2e and f. These values are higher than the sum of the adsorption and hydrogen peroxide contributions *per se*, suggesting that there is a catalytic effect in the presence of the carbon materials. It should be highlighted that during the WPO experiments the formation of benzoquinone, hydroquinone and *p*-nitrocatechol (possible intermediate by-products of PNP oxidation) was not observed. Nevertheless, it can be observed that the TOC removal is slightly lower than PNP, and this fact can be due to the possible formation of short chain carboxylic acids that contribute to the TOC. The removal performances reached by adsorption and WPO allows concluding that the carbon materials are particularly active for WPO of PNP, which was corroborated by the formation of hydroxyl radicals. Actually, Fig. 3 shows the consumption of hydrogen peroxide as a function of time and hydroxyl radicals formation in the blank run with either the support (ACM) or with the iron supported catalyst (Fe/ACM), which confirms the radicalar mechanism in both cases.

To evaluate the effect of the surface chemistry of the supports on the activity of iron catalysts in the PNP oxidation, several experiments were carried out using the different carbon supports impregnated with 2 wt.% of iron (samples Fe/ACX$_y$). Fig. 2g and h show the results of PNP and TOC reduction obtained, revealing that the surface chemistry of the carbon supports plays an important role in the Fenton's reaction. Again, Fe/ACH (sample which support exhibits the higher amount of oxygenated surface groups) presents the lowest PNP and TOC removals, and these performances increase with the decrease of the amount of oxygenated surface groups (i.e., when increasing the temperature of the heat treatment of carbon materials). The iron catalyst that presents the best performance was Fe/ACM (69.9% and 60.5% for PNP and TOC removals, respectively), which is obtained from the support with the highest N-content. The presence of N-functionalities increases the content of π-electron rich sites on their basal planes facilitating the adsorption of PNP and subsequent degradation in the presence of iron

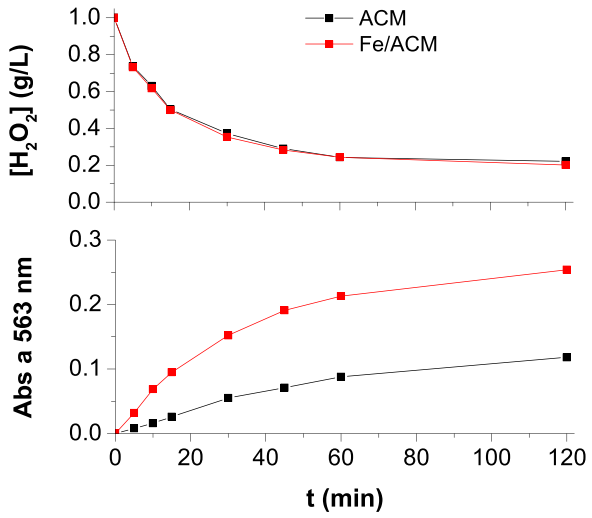

Fig. 3. Consumption of hydrogen peroxide and hydroxyl radicals formation as a function of time for experiments with the support (ACM) or with the iron supported catalyst (Fe/ACM) (pH = 3.0, T = 30 °C, [ACM] = [Fe/ACM] = 0.25 g/L, [H_2O_2] = 1.0 g/L, [PNP] = 0 mg/L).

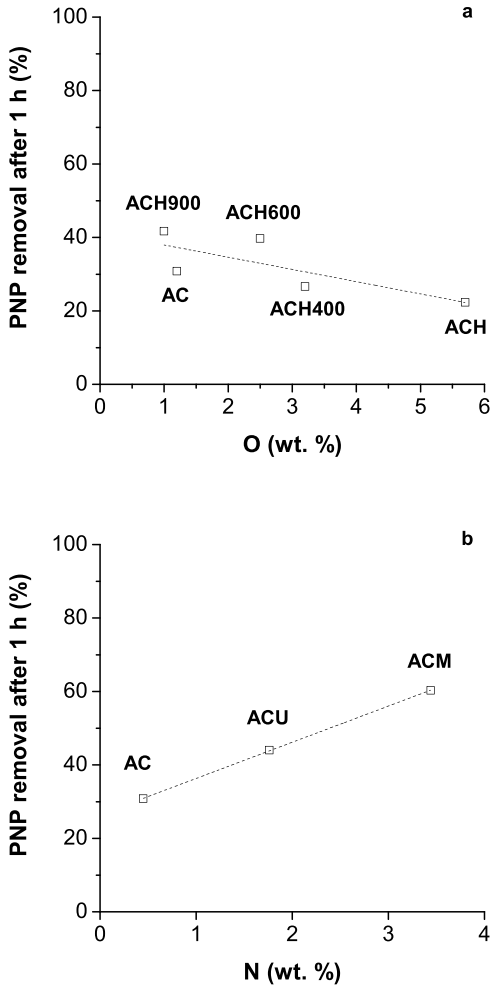

Fig. 4. Relationship between PNP removal after 1 h of Fenton reaction with the activated carbons and the percentage of oxygen in AC, ACH, ACH400, ACH600 and ACH900 supports (a) and of nitrogen in AC, ACU and ACM supports (b) (pH = 3.0, T = 30 °C, [catalyst] = 0.25 g/L, [H_2O_2] = 1.0 g/L, [PNP] = 500 mg/L).

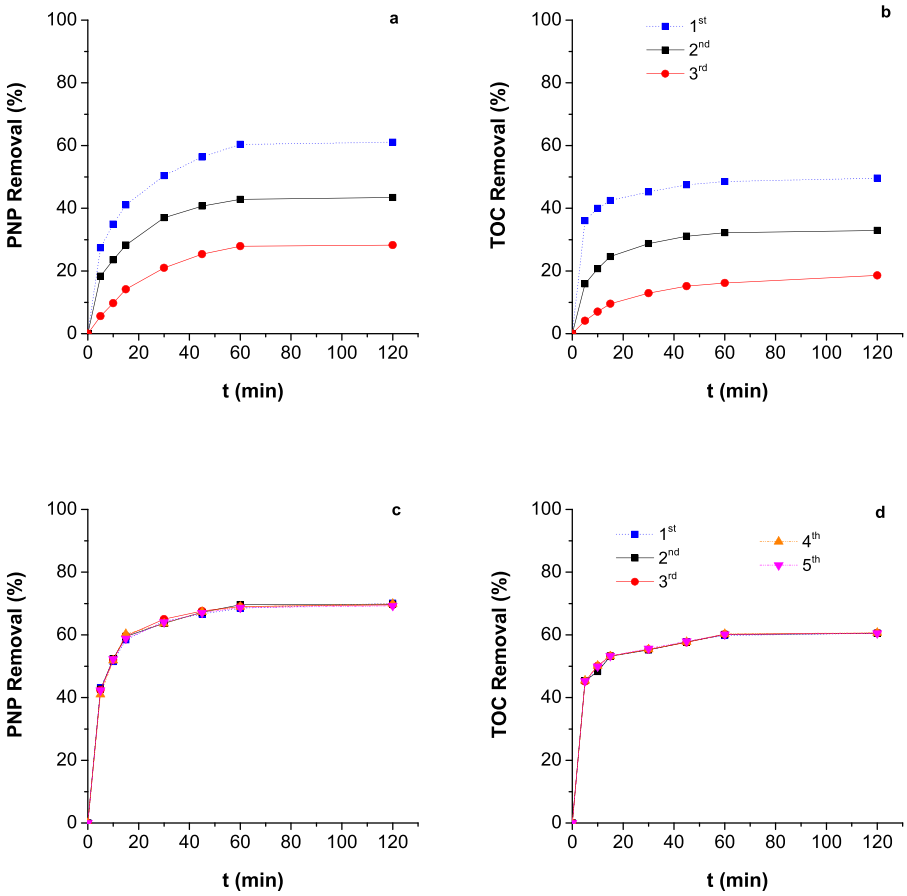

Fig. 5. PNP and TOC removal in subsequent cycles during wet peroxidation using ACM (a,b) and Fenton's reaction using Fe/ACM (c,d) (pH = 3.0, T = 30 °C, [ACM] = [Fe/ACM] = 0.25 g/L, [H_2O_2] = 1.0 g/L, [PNP] = 500 mg/L).

and H_2O_2. The highest performance of the N-doped carbon sample can be explained by the synergetic effect of the lower amount of oxygen-containing surface groups, N-functionalities and iron on the surface that favors the oxidation of the pollutants. For this catalyst the access of oxidant to the iron species can be easier because the complexing properties of N-containing groups have the ability to maintain the iron ions close to the carbon surface, comparatively to other catalysts with more oxygenated surface groups, favoring the hydroxyl radicals formation [41]. Fig. 3 shows that a larger amount of radicals was formed in the presence of the iron catalyst (Fe/ACM) than in the presence of the support ACM, for a similar consumption of oxidant, which is related to the fact that radicals are formed by two routes: i) reaction between the activated carbon and the hydrogen peroxide ($ACM + H_2O_2 \rightarrow ACM^+ + OH + HO^\bullet$ [52]) and ii) catalytic decomposition of the oxidant in the presence of iron ($ACM\text{-}Fe^{2+} + H_2O_2 \rightarrow ACM\text{-}Fe^{3+} + OH + HO^\bullet$ [15]). Zazo et al. [53] reported that the presence of iron increases the efficiency of phenol and TOC removals by catalytic peroxidation with a Fe/active carbon catalyst.

It was found that there is a relationship between the amount of oxygen (obtained by TPD – Table 4) in the thermally treated supports and the nitrogen content (measured by EA – Table 3) in the chemically (doped) modified supports and their ability to degrade PNP. A close to linear correlation between the PNP removal with the oxygen content of AC, ACH and ACH_{400}, ACH_{600} and ACH_{900} materials and with the nitrogen content of AC, ACU and ACM materials can be observed in Fig. 4a) and b), respectively, which demonstrates the important role of oxygen- and nitrogen-containing groups in the catalytic performance of the materials. The carbon material with the highest oxygen content presents the lowest catalytic activity. In contrast, the carbon material with the highest nitrogen content presents the highest catalytic activity.

3.3. Stability of the AC support and Fe/ACM catalyst

The iron catalysts only increase by ca. 10% the removal of *p*-nitrophenol and TOC when compared with the corresponding support (Fig. 2); therefore, it is relevant to assess the importance of using the iron species supported on carbon. For that, consecutive runs were performed, under the same operating conditions, to evaluate the performance of the best support and catalyst (ACM and Fe/ACM, respectively) during the oxidation of PNP. The ACM and Fe/ACM samples were recovered by filtration and used again in a subsequent run after drying at 40 °C during 1 day. Fig. 5 presents the PNP and TOC removal along time during the consecutive reaction cycles for both samples.

Fig. 5a and b show that the catalytic performance of the support ACM decreases during the reutilization cycles. This decrease is related to the porosity blocking and/or deactivation of carbon due to oxidation of its surface by the hydrogen peroxide, forming oxygen surface groups. Gomes et al. [54] and Ribeiro et al. [55] also observed the deactivation of activated carbons and carbon xerogels, respectively, when reused in a second cycle. On the other hand, in the presence of the Fe/ACM catalyst (Fig. 5c and d), no deactivation was observed and the maximum variations between the five cycles, after 2 h of reaction, are less than 0.9% and 0.3% for PNP and TOC removals, respectively. In addition, no leaching of iron was detected in all runs (detection limit of <0.2 mg/L). However, it is worth men-

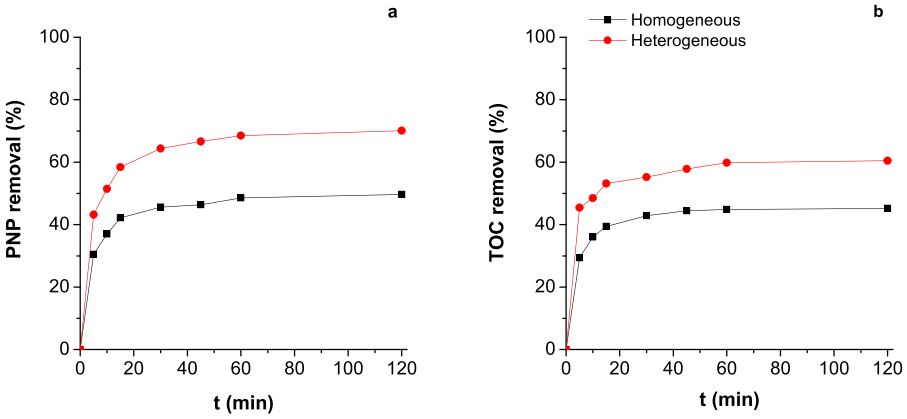

Fig. 6. PNP (a) and TOC (b) removal for homogeneous and heterogeneous Fenton process (pH = 3.0, T = 30 °C, $[Fe^{2+}]$ = 5 mg/L or [Fe/ACM] = 0.25 g/L, $[H_2O_2]$ = 1.0 g/L, [PNP] = 500 mg/L).

tioning that the catalyst, after 5 reaction cycles, still maintains its adsorption capacity: the PNP and TOC removals (both ca. 44%) are only slightly lower than those obtained with the fresh Fe/ACM (ca. 46%) and much higher than that obtained after 5 cycles of adsorption (ca. 2% for PNP and TOC removals) – data not shown. In sum, these results allowed to conclude that the presence of iron during the reaction is important making the Fe/ACM catalyst stable, which is a crucial aspect for real wastewater treatments.

3.4. Homogeneous vs. heterogeneous Fenton process

Experiments were carried out to compare the heterogeneous process with the homogeneous one. In the homogeneous assay it was used a Fe^{2+} concentration equal to the iron content in the Fe/ACM catalyst (5 mg/L). The results obtained are shown in Fig. 6 and it can be seen that the PNP and TOC removals are higher in the heterogeneous than in the homogeneous assay. Such performance wasn't anticipated, because when using the iron/activated carbon

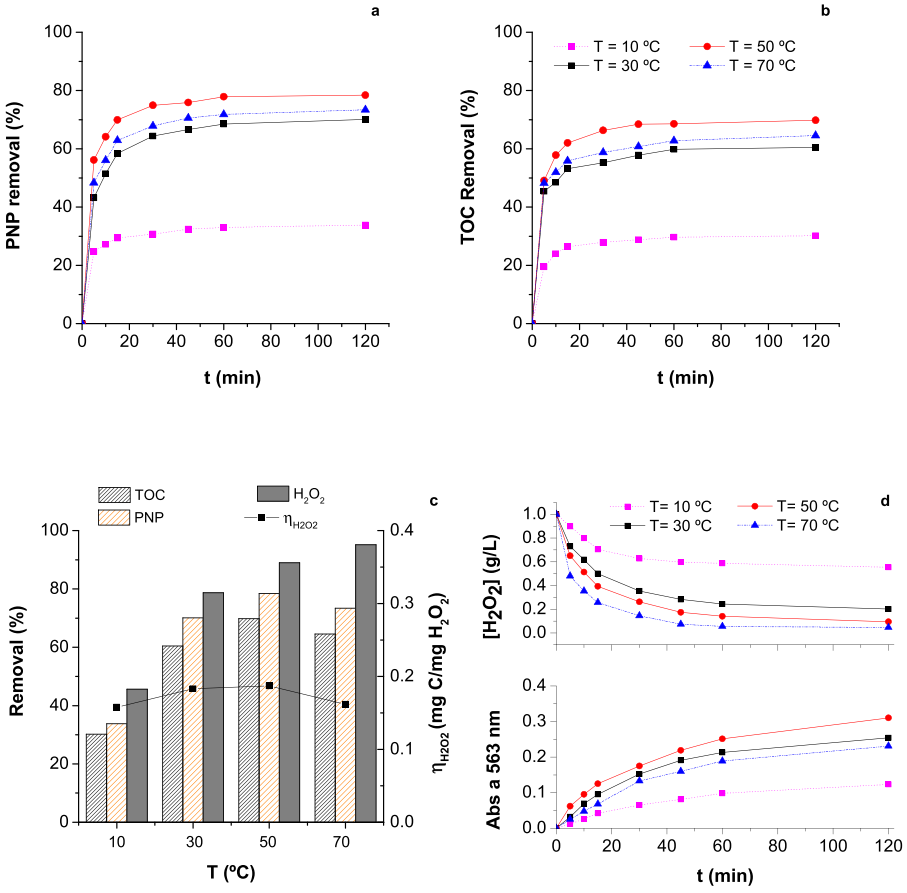

Fig. 7. Effect of temperature in PNP and TOC removal as a function of reaction time (a, b), and in TOC and PNP removal, in overall hydrogen peroxide consumption and its efficiency of use after 2 h of reaction (c), in the formation of hydroxyl radicals, and in the consumption of hydrogen peroxide in blank catalytic experiments (d) (pH = 3.0, [Fe/ACM] = 0.25 g/L, $[H_2O_2]$ = 1.0 g/L, [PNP] = 500 mg/L in a,b and c and [PNP] = 0 mg/L in d).

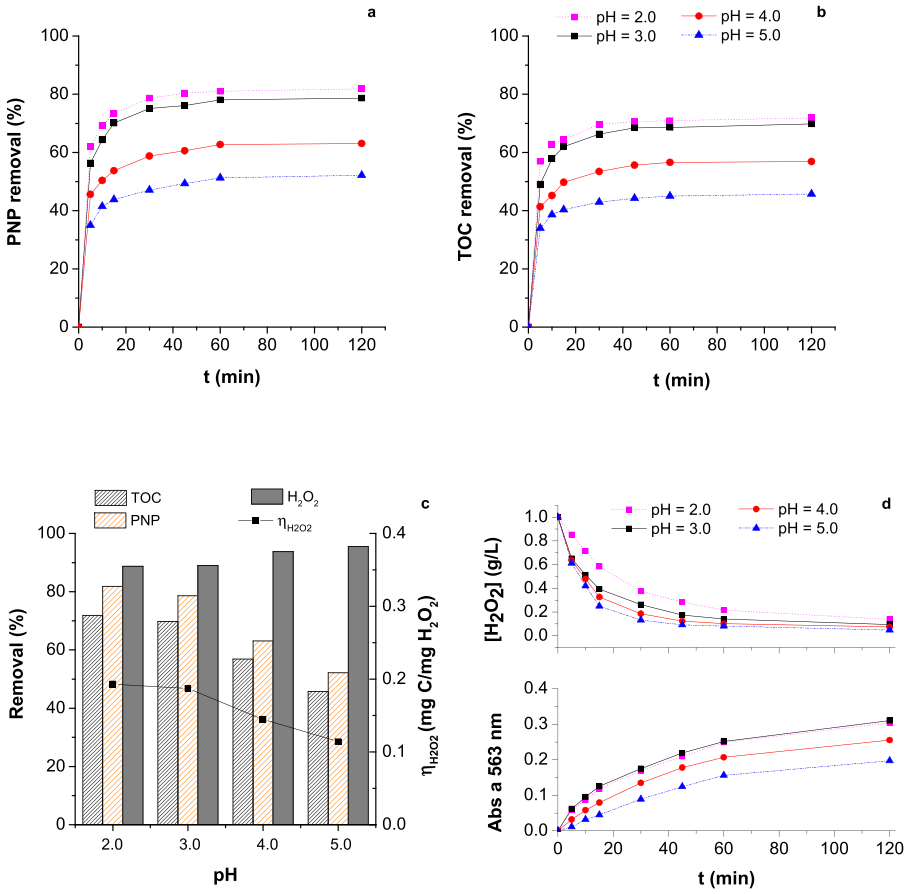

Fig. 8. Influence of pH in PNP and TOC removal as a function of reaction time (a, b), and in TOC and PNP removal, in overall hydrogen peroxide consumption and its efficiency of use after 2 h of reaction (c), in the formation of hydroxyl radicals, and in the consumption of hydrogen peroxide in blank catalytic experiments (d) (T = 50 °C, [Fe/ACM] = 0.25 g/L, $[H_2O_2]$ = 1.0 g/L, [PNP] = 500 mg/L in a, b and c and [PNP] = 0 mg/L in d).

materials the iron species are not so accessible. This increase in removals in the heterogeneous process is probably due to a synergetic process (contribution of both the support and iron species for radicals formation) and mostly to adsorption phenomena that occurs simultaneously with the Fenton reaction.

3.5. Heterogeneous Fenton's oxidation with the Fe/ACM sample

3.5.1. Effect of temperature

Since temperature is a crucial parameter in Fenton's reaction, several runs were carried out in the temperature range of 10–70 °C to evaluate its influence in PNP and TOC removal kinetics, hydrogen peroxide consumption and its efficiency of use (determined by the ratio between the amount of TOC removed and the amount of oxidant consumed – η_{H2O2} – as described elsewhere [56]).

The results obtained show that temperature has a strong effect in the process performance (see Fig. 7). PNP and TOC removals are particularly improved when the temperature was raised from 10 to 30 °C; a small improvement was observed when temperature was further increased to 50 °C, but at 70 °C the removals are detrimentally affected. The η_{H2O2} parameter after 2 h of oxidation also shows a maximum at 50 °C. The appearance of an optimum temperature was also reported by Zhang et al. [57] during degradation of PNP by heterogeneous Fenton like oxidation using acid-activated fly ash as catalyst.

The reaction rates increase with temperature (due to the increase of kinetic constants, according to Arrhenius law) but, on the other hand, for temperatures above ca. 50 °C thermal decomposition of hydrogen peroxide into water and oxygen occurs [15], which explains the worst efficiency obtained at 70 °C. This is also corroborated by the increase of H_2O_2 consumption with temperature, which does not result in increased PNP and TOC removal (see Fig. 7a, b and c). In addition, Fig. 7d shows that for the highest temperature the formation of hydroxyl radicals is reduced in spite of the higher consumption of oxidant as compared to runs carried out at 30–50 °C. The optimum temperature found in this work is equal to that reached by Zazo et al. [53] for phenol removal by wet peroxidation using Fe/Ac as catalyst. For all temperatures tested no iron leaching in solution was detected.

3.5.2. Effect of pH

The Fenton reaction usually occurs in acidic medium (pH 2–4), which facilitates the production of hydroxyl radicals [58]. Thus, assays at pH values between 2.0 and 5.0 were carried out to evaluate the influence of this parameter. Fig. 8 shows that the highest PNP and TOC removals were reached at pH values around 2.0-3.0, which is related with the higher efficiency of hydrogen peroxide use (see Fig. 8c). These optima pH values are similar to those obtained in studies reported in the literature when treating PNP with limonite [59] or when removing other pollutants by wet peroxidation using carbon [60] or carbon impregnated with iron [53] as catalysts. As expected, a decrease in PNP and TOC conversion with pH values greater than 3 was observed, due to the lower stability of hydrogen peroxide, which decomposes into molecular oxygen instead of being used for the generation of radicals. In fact, Fig. 8c shows that the highest consumption of H_2O_2 at higher pHs does not provide better PNP and TOC removals, while Fig. 8d shows the decrease of hydroxyl radicals in solution for pHs higher than 3.0. Moreover,

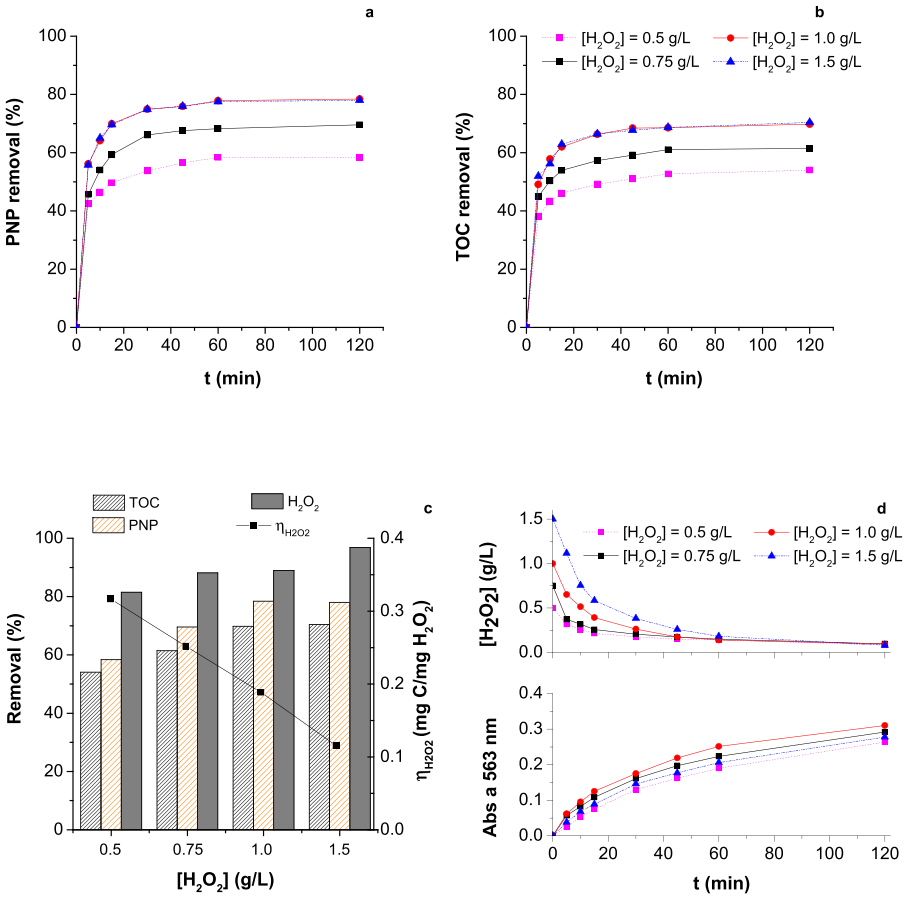

Fig. 9. Influence of H_2O_2 concentration in PNP and TOC removal as a function of reaction time (a, b), and in TOC and PNP removal, in overall hydrogen peroxide consumption and its efficiency of use after 2 h of reaction (c), in the formation of hydroxyl radicals, and in the consumption of hydrogen peroxide in blank catalytic experiments (d) (T = 50 °C, pH = 3.0, [Fe/ACM] = 0.25 g/L, [PNP] = 500 mg/L in a, b and c and [PNP] = 0 mg/L in d).

the hydroxyl radicals oxidation potential also decreases with pH increase (2.65–2.80 at pH = 3 and 1.90 V at pH = 7) [61].

For pH = 2.0 an iron concentration of 0.9 mg Fe/L was measured due to leaching, but for higher pH values no iron was detected in solution. Taking into account the occurrence of leaching at pH = 2.0, which ultimately leads to catalyst deactivation, the pH = 3.0 was chosen as the optimum for further experiments.

3.5.3. *Effect of the hydrogen peroxide concentration*

Hydrogen peroxide is the hydroxyl radicals source, and thus its concentration influences the degradation of PNP and other organic matter formed during the Fenton's oxidation. In this study the dose of oxidant was varied between 0.5 and 1.5 g/L.

The results of PNP removal and mineralization along the120 min of reaction are, respectively, shown in Fig. 9a and b, while the overall removals, the hydrogen peroxide consumption and efficiency of use after 2 h of reaction are reported in Fig. 9c. It was observed that the PNP and TOC removal increase with the dose of oxidant, up to 1.0 g/L, and remain nearly constant for higher oxidant concentration. This indicates that there is an optimum dose of hydrogen peroxide, as already reported by other authors for the degradation of PNP by Fenton oxidation [57,62] and other pollutants by heterogeneous Fenton oxidation using Fe/AC as catalysts [50] or by wet peroxidation with activated carbon [60]. The existence of an optimum oxidant dose can be explained by the parallel and undesirable scavenging of the hydroxyl radicals that may occur, leading to their consumption by the H_2O_2 ($HO^\bullet + H_2O_2 \rightarrow H_2O + HO_2^\bullet$ [15]), thus decreasing the number of radicals available to oxidize the organic matter; although perhydroxyl radicals are formed, their oxidation potential is much smaller than that of the hydroxyl radicals. This explanation is also supported by the nearly complete conversion of H_2O_2 shown in Fig. 9c for doses higher than 1.0 g/L, for which PNP and TOC removals do not increase. Also Fig. 9d (blank runs) shows that although the conversion rate of H_2O_2 is accelerated for higher hydrogen peroxide amounts (experiment with 1.5 g/L), a higher concentration of radicals is not observed (i.e. the absorbance at 563 nm, in the presence of 1,5-diphenyl carbazide, does not increase with the initial H_2O_2 concentration). It is worth noting that the optimal dose of oxidant is only ca. 59% of the stoichiometric amount required for total degradation of 500 mg/L of PNP – 1.7 g/L ($C_6H_5NO_3 + 14H_2O_2 \rightarrow 6CO_2 + 16H_2O + HNO_3$). However, the overall TOC reduction was higher than such a value, which is related to the fact that its removal occurs not only by oxidation but also by adsorption, as shown before.

The efficiency of use of the oxidant decreases with the increase of hydrogen peroxide concentration, which indicates that the consumption of more oxidant is not effectively used in the mineralization. This was supported by the fact that an increase in the dose from 500 mg/L (minimal concentration tested) to 1.0 g/L, (dose that maximizes the PNP and TOC removals), i.e. duplicating the dose, does not imply the same increase in the removal efficiency (Fig. 9c) and radicals formation (Fig. 9d). Therefore, considering the maximization of the pollutant removal and mineralization, the optimum dose was considered to be 1.0 g/L. For all doses of oxidant tested no iron leached was detected in solution.

3.5.4. *Effect of the catalyst dose*

To evaluate the influence of catalyst concentration in PNP and TOC removal, five experiments were performed varying the Fe/ACM amount in the range 0.25–3.0 g/L (corresponding to overall iron

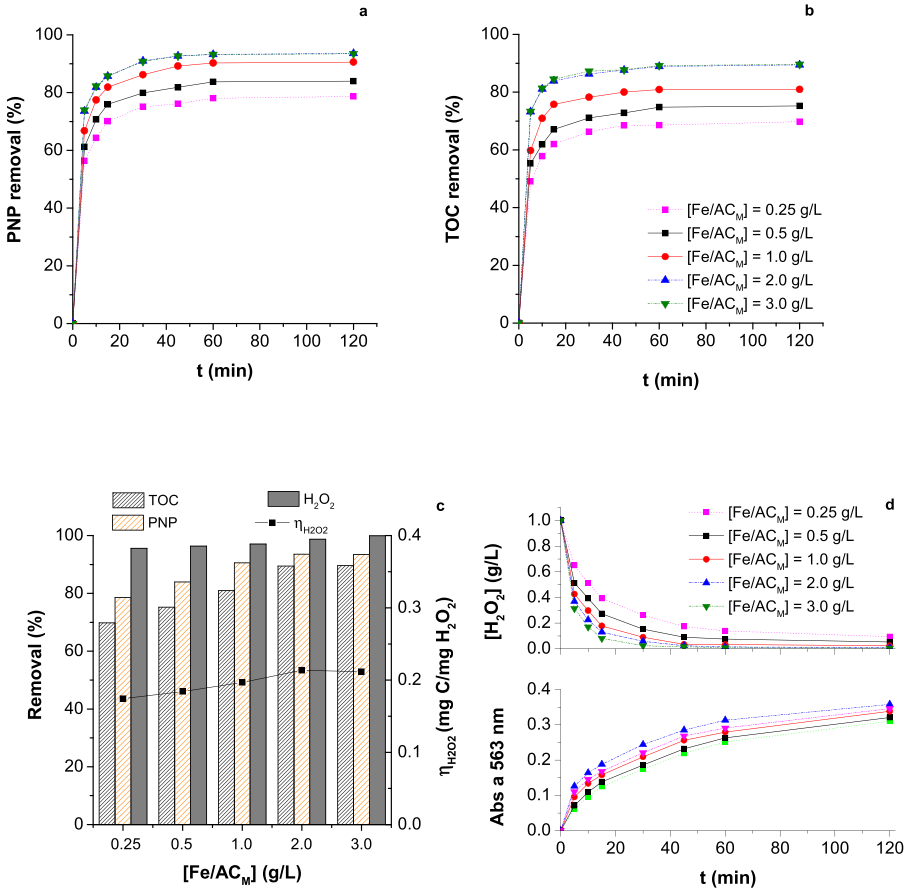

Fig. 10. Effect of catalyst dose in PNP and TOC removal as a function of reaction time (a, b), and in TOC and PNP removal, in overall hydrogen peroxide consumption and its efficiency of use after 2 h of reaction (c), in the formation of hydroxyl radicals, and in the consumption of hydrogen peroxide in blank catalytic experiments (d) (T = 50 °C, pH = 3.0, [H_2O_2] = 1.0 g/L, [PNP] = 500 mg/L in a, b and c and [PNP] = 0 mg/L in d).

concentrations between 5 and 60 mg/L). Fig. 10a and b present the PNP and TOC removals during reaction and Fig. 10c presents these removals, oxidant consumption and η_{H2O2} after 2 h of reaction. The results obtained allow concluding that the PNP and TOC removals, as well as the efficiency of oxidant use (assessed by η_{H2O2}), increase with the Fe/ACM dose up to 2.0 g/L (40 mg/L of iron) and then remain nearly constant.

Concerning either PNP or organic matter removal by Fenton's oxidation, optimum doses of catalyst are often reported in the literature [22,57,59,63], which is explained by the detrimental effect of excessive catalyst dosages leading to competitive reactions ($Fe^{2+} + HO^{\bullet} \rightarrow Fe^{3+} + HO^{-}$ [15]) that reduce the amount of radicals available. This is corroborated by the highest consumption of hydrogen peroxide observed for the catalyst concentration of 3.0 g/L (Fig. 10c), which does not result in an increase of the process efficiency. On other hand, this results in lower formation of radicals and higher consumption of hydrogen peroxide in runs without pollutant for [Fe/ACM] = 3.0 g/L – see Fig. 10d.

The optimal dose of iron (40 mg/L) found in this work, to treat a PNP solution with 500 mg/L, is much lower than those reported in other studies that used 363 mg/L [62] and 201 mg Fe/L [57] to oxidize PNP in the concentration ranges 25–45 mg/L and 100 mg/L, respectively.

Again, no leaching of iron was noticed (or else it was smaller than the detection limit of <0.2 mg/L), even for the highest dose of catalyst employed.

3.5.5. *Evaluation of toxicity, biodegradability and intermediates compounds*

After evaluating the influence of each operating condition in the degradation of PNP by the heterogeneous Fenton process,

Table 5
Concentration of PNP and intermediate compounds along the experiment under optimized conditions, total carbon based on such analyzed compounds, experimental TOC and carbon balance.

t (min)	PNP (mgC/L)	Pyruvic (mgC/L)	Maleic (mgC/L)	Oxalic (mgC/L)	Acetic (mgC/L)	Total carbon[a] (mgC/L)	TOC (mgC/L)	Contribution[b] (%)
0	257.9	0.0	0.0	0.0	0.0	257.9	251.7	100.0
5	67.5	0.0	0.0	0.0	0.0	67.5	70.9	95.3
10	46.6	2.1	1.7	1.4	0.0	51.8	52.3	99.2
15	36.8	2.8	3.0	2.4	0.0	44.8	44.9	100.0
30	22.9	6.0	5.1	5.1	0.0	39.1	39.2	99.9
45	18.5	3.9	3.3	6.2	2.9	34.9	35.4	98.5
60	16.9	2.8	2.0	7.1	3.7	32.6	32.9	99.2
120	16.0	2.2	1.6	6.3	3.0	29.1	31.2	93.1

[a] Total carbon assessed from the sum of the identified compounds.
[b] Total carbon/TOC x 100.

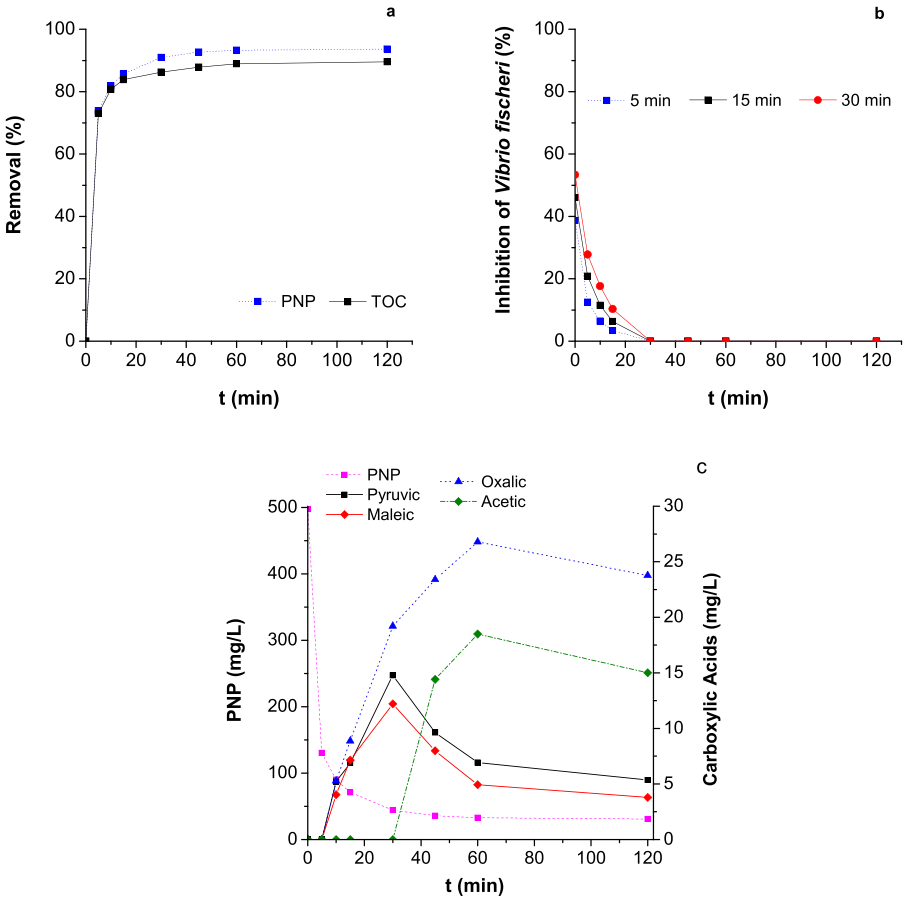

Fig. 11. PNP and TOC removals (a), inhibition of *Vibrio Fischeri* for different contact times of the effluent with the bacteria (b) and PNP and carboxylic acids concentration (c) as a function of reaction time under optimized conditions (T = 50 °C, pH = 3.0, $[H_2O_2]$ = 1.0 g/L, [Fe/ACM] = 2.0 g/L, [PNP] = 500 mg/L).

another experiment was carried out using the optimum operating conditions determined in the previous sections: pH = 3.0, T = 50 °C, $[H_2O_2]$ = 1.0 g/L and [Fe/ACM] = 2.0 g/L. Under these conditions, the PNP, TOC and COD removals achieved were 93.6, 87.6 and 85.7%, respectively, after 2 h of reaction (replicate of this experiment provided variations <2%). High consumption of H_2O_2 was reached (98.7%), with an efficiency of oxidant use (η_{H2O2}) of 0.23 mgC/mgH_2O_2. The biodegradability of the effluent was quantified by the BOD_5:COD ratio and BOD_5, which increased from <0.001 to 0.36 and <1.0 to 42 mgO_2/L, respectively.

Regarding the toxicity of the effluent, measured by the inhibition of *Vibrio fischer*i, a significant decrease was observed in the first 5 min of reaction, which corresponds to significant removals of PNP and TOC, as shown in Fig. 11a and b. The inhibition decreases continuously, although more slowly thereafter, till 30 min of reaction, and then a non-toxic effluent was generated (0.0%). Once more, no iron was detected in solution (<0.2 mg/L).

In this run the intermediate compounds formed during the reaction were identified and quantified. In the first 5 min of reaction no intermediate compounds were detected and the total organic carbon measured corresponds to the concentration of PNP in solution as shown in Table 5. After 10 min of reaction the formation of maleic, pyruvic and oxalic acid was observed, whose concentrations increase with time until 30 min (see also Fig. 10c). After this period the concentration of maleic and pyruvic acids decays, possibly due to their oxidation into oxalic and acetic acids, respectively, as proposed in the works developed by Sun et al. [62] and Li et al. [64]. The concentration of these carboxylic acids increased with reaction time up to 60 min, decreasing later on (possibly due to their mineralization). The concentration of oxalic and acetic acid slightly decays for a reaction time of 120 min since they were not generated (no further degradation of PNP occurs) and also occurs degradation by hydroxyl radicals to carbon dioxide and water, as reported in others studies [62,64]. In this reaction, the higher molecular weight intermediates (nitrocatechol, benzoquinone and hydroquinone) that would be the first compounds formed, according to other studies reported in the literature [62], were not detected probably because they are easily degraded into carboxylic acids. This fact was supported by the carbon balance which was not closed at 100% (although was higher than 94% – see Table 5).

4. Conclusions

PNP was used as model recalcitrant compound and it was observed that the surface chemical properties of the carbon supports play an important role in their adsorption and/or catalytic properties. The carbon support (ACH) or the iron catalyst (Fe/ACH) supported on the carbon sample with the highest amount of oxygenated surface groups present the worst performances for adsorption or Fenton's oxidation. The performance of the processes increases with the removal of these oxygenated surface groups, the highest removals being obtained with the carbon samples with lower content of oxygenated surface groups. However, the carbon sample N-doped with melamine (with the highest amount of N-functionalities) presented enhanced performances for the removal of PNP. A relationship between the PNP removal with the oxygen and nitrogen content of the materials was found, demonstrating the important role of oxygen- and nitrogen-containing groups in the catalytic performance of the materials.

The heterogeneous Fenton's oxidation proved to be a promising technique for the degradation of PNP using Fe/ACM as catalyst. This material shows to be very stable during reutilization runs without any iron leaching, which is crucial for its industrial application, which requires testing under continuous operation. High removals of PNP, TOC and COD (94, 90 and 86%, respectively) were achieved after 2 h of reaction with the optimized operation conditions (pH = 3.0, T = 50 °C, $[H_2O_2]$ = 1.0 g/L and [Fe/ACM] = 2.0 g/L). A high consumption of hydrogen peroxide (98.7%) was also reached, while a more biodegradable (BOD_5:COD ratio increased from <0.001 to 0.36) and non-toxic effluent was generated.

Acknowledgments

This work was financially supported by Project POCI-01-0145-FEDER-006939 (Laboratory for Process Engineering, Environment, Biotechnology and Energy – LEPABE) funded by FEDER funds through COMPETE2020 – Programa Operacional Competitividade e Internacionalização (POCI) – and by national funds through FCT - Fundação para a Ciência e a Tecnologia. Carmen Rodrigues is grateful to LEPABE for financial support through the Post-doctoral grant. This work was also partially funded by project "AIProcMat@N2020 – Advanced Industrial Processes and Materials for a Sustainable Northern Region of Portugal 2020", with the reference NORTE-01-0145-FEDER-000006, supported by Norte Portugal Regional Operational Programme (NORTE 2020), under the Portugal 2020 Partnership Agreement, through the European Regional Development Fund (ERDF) and of Project POCI-01-0145-FEDER-006984–Associate Laboratory LSRE-LCM funded by ERDF through COMPETE2020 – Programa Operacional Competitividade e Internacionalização (POCI) – and by national funds through FCT – Fundação para a Ciência e a Tecnologia.

References

[1] ATSDR, Toxicological Profile for Nitrophenols: 2-Nitrophenol and 4-Nitrophenol, Public Agency for Toxic Substances and Disease Registry, Health Service, 1992.
[2] USEPA, National Pesticide Survey: 4-NitroPhenol, National Service Center for Environmental Publications, 2015, 2017.
[3] U.S.EPA, 4-Nitrophenol, in: H.a.E.E.P.N. 135 (Ed.), Government Printing Office, District of Columbia, U.S., 1980.
[4] Z. Jia, M. Jiang, G. Wu, Chem. Eng. J. 307 (2016) 283–290.
[5] F. Liu, Z. Wu, D. Wang, J. Yu, X. Jiang, X. Chen, Colloids Surf. A: Physicochem. Eng. Aspects 490 (2016) 207–214.
[6] D. Chen, K. Yang, L. Wei, H. Wang, Bioresour. Technol. 218 (2016) 189–195.
[7] M. Martín-Hernández, M.E. Suárez-Ojeda, J. Carrera, Bioresour. Technol. 123 (2012) 150–156.
[8] M. Zhou, L. Lei, Chemosphere 65 (2006) 1197–1203.
[9] F. Xie, Y. Xu, K. Xia, C. Jia, P. Zhang, Ultrason. Sonochem. 28 (2016) 199–206.
[10] Q. Ji, J. Li, Z. Xiong, B. Lai, Chemosphere 172 (2017) 10–20.
[11] L. Tang, J. Tang, G. Zeng, G. Yang, X. Xie, Y. Zhou, Y. Pang, Y. Fang, J. Wang, W. Xiong, Appl. Surf. Sci. 333 (2015) 220–228.
[12] P. Cañizares, R. Paz, C. Sáez, M.A. Rodrigo, J. Environ. Manage. 90 (2009) 410–420.
[13] A.E. Papadopoulos, D. Fatta, M. Loizidou, J. Hazard. Mater. 146 (2007) 558–563.
[14] J. Kiwi, C. Pulgarin, P. Peringer, Appl. Catal. B: Environ. 3 (1994) 335–350.
[15] C. Walling, Acc. Chem. Res. 8 (1975) 125–131.
[16] M. Cheng, G. Zeng, D. Huang, C. Lai, P. Xu, C. Zhang, Y. Liu, J. Wan, X. Gong, Y. Zhu, J. Hazard. Mater. 312 (2016) 184–191.
[17] A.M. Mesquita, I.R. Guimarães, G.M.M.d. Castro, M.A. Gonçalves, T.C. Ramalho, M.C. Guerreiro, Appl. Catal. B: Environ. 192 (2016) 286–295.
[18] X. Huang, X. Hou, J. Zhao, L. Zhang, Appl. Catal. B: Environ. 181 (2016) 127–137.
[19] S.A. Messele, Soares O.S.G.P, J.J.M. Órfão, C. Bengoa, F. Stüber, A. Fortuny, A. Fabregat, J. Font. Catal. Today 240 (2015) 73–79.
[20] C.M. Domínguez, A. Quintanilla, P. Ocón, J.A. Casas, J.J. Rodriguez, Carbon 60 (2013) 76–83.
[21] F. Stüber, J. Font, A. Fortuny, C. Bengoa, A. Eftaxias, A. Fabregat, Top. Catal. 33 (2005) 3–50.
[22] F. Duarte, V. Morais, F.J. Maldonado-Hódar, L.M. Madeira, J. Chem. Eng. 232 (2013) 34–41.
[23] B.M. Esteves, C.S.D. Rodrigues, R.A.R. Boaventura, F.J. Maldonado-Hódar, L.M. Madeira, J. Environ. Manage. 166 (2016) 193–203.
[24] F. Duan, Y. Yang, Y. Li, H. Cao, Y. Wang, Y. Zhang, J. Environ. Sci. 26 (2014) 1171–1179.
[25] N. Ferroudj, J. Nzimoto, A. Davidson, D. Talbot, E. Briot, V. Dupuis, A. Bée, M.S. Medjram, S. Abramson, Appl. Catal. B: Environ. 136–137 (2013) 9–18.
[26] D. Wan, W. Li, G. Wang, L. Lu, X. Wei, Sci. Total Environ. 574 (2017) 1326–1334.
[27] X. Sun, L. Sun, Y. Zheng, Q. Lin, H. Su, F. Li, C. Qi, Synth. Met. 220 (2016) 635–642.
[28] Y. Zhong, X. Liang, Z. He, W. Tan, J. Zhu, P. Yuan, R. Zhu, H. He, Appl. Catal. B: Environ. 150–151 (2014) 612–618.
[29] O.S.G.P. Soares, J.J.M. Órfão, E. Gallegos-Suarez, E. Castillejos, I. Rodríguez-Ramos, M.F.R. Pereira, Environ. Technol. 33 (2012) 2353–2358.
[30] Z.I. Bhatti, H. Toda, K. Furukawa, Water Res. 36 (2002) 1135–1142.
[31] A.APHA, WEF, Standard Methods for the Examination of Water and Wastewater, American Public Health Association, American Water Works Association, Water Pollution Control Federation, Washington, DC, 1998.
[32] R.M. Sellers, Analyst 105 (1980) 950–954.
[33] J. Wang, Y. Guo, J. Gao, X. Jin, Z. Wang, B. Wang, K. Li, Y. Li, Ultrason. Sonochem. 18 (2011) 1028–1034.
[34] I.O.f. Standardization, Water Quality –Determination of the Inhibitory Effect of Water Samples on the Light Emission of Vibrio Fischeri (luminescent Bacteria Test), 2005.
[35] J. Jaramillo, P.M. Álvarez, V. Gómez-Serrano, Fuel Process. Technol. 91 (2010) 1768–1775.
[36] J.L. Figueiredo, M.F.R. Pereira, M.M.A. Freitas, J.J.M. Orfao, Carbon 37 (1999) 1379–1389.
[37] E. Vega, J. Lemus, A. Anfruns, R. Gonzalez-Olmos, J. Palomar, M.J. Martin, J. Hazard. Mater. 258–259 (2013) 77–83.
[38] A. Rey, A.B. Hungria, C.J. Duran-Valle, M. Faraldos, A. Bahamonde, J.A. Casas, J.J. Rodriguez, Appl. Catal. B: Environ. 181 (2016) 249–259.
[39] M.F.R. Pereira, S.F. Soares, J.J.M. Órfão, J.L. Figueiredo, Carbon 41 (2003) 811–821.
[40] A. Rey, J.A. Zazo, J.A. Casas, A. Bahamonde, J.J. Rodriguez, Appl. Catal. A: Gen. 402 (2011) 146–155.
[41] S.A. Messele, Soares O.S.G.P, J.J.M. Órfão, F. Stüber, C. Bengoa, A. Fortuny, A. Fabregat, J. Font, Appl. Catal. B: Environ. 154–155 (2014) 329–338.
[42] Y. Gokce, Z. Aktas, Appl. Surf. Sci. 313 (2014) 352–359.
[43] J.L. Figueiredo, M.F.R. Pereira, M.M.A. Freitas, J.J.M. Órfão, Ind. Eng. Chem. Res. 46 (2007) 4110–4115.
[44] V. Priyanka, V.C. Subbaramaiah, I.D. Srivastava, Sep. Mall, Purif. Technol. 125 (2014) 284–290.
[45] O.S.G.P. Soares, J.J.M. Órfão, M.F.R. Pereira, Ind. Eng. Chem. Res. 49 (2010) 7183–7192.
[46] A. Rey, M. Faraldos, J.A. Casas, J.A. Zazo, A. Bahamonde, J.J. Rodríguez, Appl. Catal. B: Environ. 86 (2009) 69–77.
[47] J.X. Guo, X.L. Liu, D.M. Luo, H.Q. Yin, J.J. Li, Y.H. Chu, Ind. Eng. Chem. Res. 54 (2015) 1261–1270.
[48] X. Mou, Y. Li, B. Zhang, L. Yao, X. Wei, D.S. Su, W. Shen, Eur. J. Inorg. Chem. (2012) 2684–2690.
[49] C. Moreno-Castilla, J. Rivera-Utrilla, M.V. López-Ramón, F. carrasco-Marín, Carbon 33 (1995) 845–851.
[50] A. Dhaouadi, N. Adhoum, Appl. Catal. B: Environ. 97 (2010) 227–235.
[51] R.S. Ribeiro, A.M.T. Silva, J.L. Figueiredo, J.L. Faria, H.T. Gomes, Appl. Catal. B: Environ. 140–141 (2013) 356–362.
[52] Y. Wang, H. Wei, P. Liu, Y. Yu, Y. Zhao, X. Li, W. Jiang, J. Wang, X. Yang, C. Sun, Catal. Today 258 (Part 1) (2015) 120–131.
[53] J.A. Zazo, J.A. Casas, A.F. Mohedano, J.J. Rodríguez, Appl. Catal. B: Environ. 65 (2006) 261–268.
[54] H.T. Gomes, S.M. Miranda, M.J. Sampaio, A.M.T. Silva, J.L. Faria, Catal. Today 151 (2010) 153–158.
[55] R.S. Ribeiro, N.A. Fathy, A.A. Attia, A.M.T. Silva, J.L. Faria, H.T. Gomes, Chem. Eng. J. 195–196 (2012) 112–121.
[56] I.F. Mena, E. Diaz, J.J. Rodriguez, A.F. Mohedano, J. Chem. Eng. 318 (2017) 153–160.
[57] A. Zhang, N. Wang, J. Zhou, P. Jiang, G. Liu, J. Hazard. Mater. 201–202 (2012) 68–73.
[58] E. Neyens, J. Baeyens, J. Hazard. Mater. 98 (2003) 33–50.
[59] H.-C. Tao, X.-Y. Wei, L.-J. Zhang, T. Lei, N. Xu, J. Hazard. Mater. 254–255 (2013) 236–241.
[60] H.T. Gomes, S.M. Miranda, M.J. Sampaio, J.L. Figueiredo, A.M.T. Silva, J.L. Faria, Appl. Catal. B: Environ. 106 (2011) 390–397.
[61] A. Chen, X. Ma, H. Sun, J. Hazard. Mater. 156 (2008) 568–575.
[62] S.-P. Sun, A.T. Lemley, J. Mol. Catal. A: Chem. 349 (2011) 71–79.
[63] W. Wang, Y. Liu, T. Li, M. Zhou, J. Chem. Eng. 242 (2014) 1–9.
[64] W. Li, Z. Qiang, T. Zhang, X. Bao, X. Zhao, J. Mol. Catal. A: Chem. 348 (2011) 70–76.